

Closed-system behaviour of the Re–Os isotope system recorded in primary and secondary platinum-group mineral assemblages: Evidence from a mantle chromitite at Harold's Grave (Shetland Ophiolite Complex, Scotland)



Inna Yu. Badanina ^a, Kreshimir N. Malitch ^{a,c,*}, Richard A. Lord ^b, Elena A. Belousova ^c, Thomas C. Meisel ^d

^a Department of Geochemistry and Ore-Forming Processes, A.N. Zavaritsky Institute of Geology and Geochemistry, the Uralian Branch of Russian Academy of Sciences, Pochtovy per. 7, Ekaterinburg 620075, Russia

^b Department of Civil and Environmental Engineering, University of Strathclyde, Glasgow G4 0NG, United Kingdom

^c ARC Centre of Excellence for Core to Crust Fluid Systems/GEMOC Key Centre, Department of Earth and Planetary Sciences, Macquarie University, Sydney, NSW 2109, Australia

^d Department of General and Analytical Chemistry, University of Leoben, Leoben 8700, Austria

ARTICLE INFO

Article history:

Received 24 July 2015

Received in revised form 8 December 2015

Accepted 14 December 2015

Available online 17 December 2015

Keywords:

Platinum-group minerals

Chromitite

Osmium isotopes

Mantle

Harold's Grave

Shetland Ophiolite Complex

ABSTRACT

This study evaluates in detail the mineral chemistry, whole-rock and mineral separate Os-isotope compositions of distinct platinum-group mineral (PGM) assemblages in an isolated chromitite pod at Harold's Grave which occurs in mantle tectonite in the Shetland Ophiolite Complex (SOC), Scotland. This was the first ophiolite sequence worldwide that was shown to contain ppm levels of all six platinum-group elements (PGE) in podiform chromitite, including the contrasting type localities found here and at Cliff. At Harold's Grave the primary PGM assemblage is composed mainly of laurite and/or Os-rich iridium and formed early together with chromite, whereas the secondary PGM assemblage dominated by laurite, Os-rich laurite, irarsite, native osmium and Ru-bearing pentlandite is likely to reflect processes including in-situ serpentization, alteration during emplacement and regional greenschist metamorphism. The osmium isotope data define a restricted range of 'unradiogenic' $^{187}\text{Os}/^{188}\text{Os}$ values for coexisting laurite and Os-rich alloy pairs from 'primary' PGM assemblage (0.12473–0.12488) and similar 'unradiogenic' $^{187}\text{Os}/^{188}\text{Os}$ values for both 'primary' and 'secondary' PGM assemblages (0.1242 ± 0.0008 and 0.1245 ± 0.0006 , respectively), which closely match the bulk $^{187}\text{Os}/^{188}\text{Os}$ value of their host chromitite (0.1240 ± 0.0006). The unprecedented isotopic similarity between primary or secondary PGM assemblages and chromitite we report suggests that the osmium isotope budget of chromitite is largely controlled by the contained laurite and Os-rich alloy. This demonstrates that closed system behaviour of the Re–Os isotope system is possible, even during complex postmagmatic hydrothermal and/or metamorphic events. The preserved mantle Os-isotope signatures provide further support for an Enstatite Chondrite Reservoir (ECR) model for the convective upper mantle and are consistent with origin of the complex as a Caledonian ophiolite formed in a supra-subduction zone setting shortly before obduction.

© 2015 Elsevier B.V. All rights reserved.

1. Introduction

Osmium isotopes are considered as important tracers for understanding the evolution of highly siderophile elements (HSE) in the upper mantle. Due to the progress of analytical techniques in recent years, the Re–Os system has been widely applied for evaluating distinct mantle sources and dating melting events in the mantle in different

geological settings (see Shirey and Walker, 1998; Carlson, 2005; Rudnick and Walker, 2009 and references therein). In contrast to the geochemical properties of strontium, neodymium, hafnium, and lead, all of which are incompatible elements, osmium behaves as compatible element during mantle melting processes leading to high Os contents in the residual mantle (Barnes et al., 1985; Hart and Ravizza, 1996; Burton et al., 1999, 2002, among others).

Although considered more robust than lithophile element based isotopic systems, it was suggested that the Re–Os isotopic system is not entirely immune to resetting and disruptions (Brandon et al., 1996; Becker et al., 2001; Le Roux et al., 2009; O'Reilly and Griffin, 2012 and references therein). Ambiguity in the use and interpretation of whole rock Os isotope data also arose from a number of mineral-scale Os-isotopic studies (Burton et al., 1999; Alard et al., 2002, 2005, etc.), which proved

* Corresponding author at: Department of Geochemistry and Ore-Forming Processes, A.N. Zavaritsky Institute of Geology and Geochemistry, the Uralian Branch of Russian Academy of Sciences, Pochtovy per. 7, Ekaterinburg 620075, Russia.

E-mail addresses: innabandanina@yandex.ru (I.Y. Badanina), dunite@yandex.ru (K.N. Malitch), richard.lord@strath.ac.uk (R.A. Lord), elena.belousova@mq.edu.au (E.A. Belousova), thomas.meisel@unileoben.ac.at (T.C. Meisel).

the existence of inter-mineral ‘Os-heterogeneity’ within individual samples. These studies showed that the unradiogenic Os isotopic signature of base-metal sulphides enclosed in silicate can easily be masked by external highly radiogenic secondary BM sulphides and thus cannot be estimated from whole rock Os isotopes alone. This necessitates careful evaluation of different mineral phases to evaluate the significance of the whole rock Re–Os isotope signatures and model ages (Reisberg et al., 2004). The Os isotopic system of minerals such as chromite, olivine, base-metal sulphide, Ru–Os sulphide and Os-rich alloy may contribute to a better understanding and more accurate interpretation of the processes that govern the behaviour of Os isotopes in different mantle environments (Hattori and Hart, 1991; Burton et al., 1999; Standish et al., 2001; Alard et al., 2002, 2005; Walker et al., 2002b; Malitch et al., 2003a; Ahmed et al., 2006; Brandon et al., 2006; Pearson et al., 2007; Shi et al., 2007; Nowell et al., 2008; Marchesi et al., 2011; Badanina et al., 2014; González-Jiménez et al., 2014; Luguet et al., 2015). Primary Os-bearing PGM (laurite–erlichmanite series, RuS_2 – OsS_2 and Ru–Os–Ir alloys) that form inclusions in chromite are particularly important because these are well protected by the host mineral and presumably preserve initial Os isotope values of the source Ru–Os sulphides and Ru–Os–Ir alloys were crystallized. The Os budget of the mantle is mainly controlled by sulphides and alloys (Martin et al., 1993; Hart and Ravizza, 1996; Burton et al., 1999) so combining micro-analysis of both Os-bearing sulphides and alloys, coupled with whole rock data, offers a way to test for intra-sample heterogeneity and hence allows a more robust interpretation of the Os-isotope systematics.

Two contrasting types of PGM suite are known to occur in podiform chromitites from within the mantle sequence of the Shetland Ophiolite Complex (SOC). These include both IPGE- (i.e., Os, Ir, Ru) and PPGE- (Rh, Pt, Pd) rich assemblages, which are exemplified by two type localities, referred to by the nearby place names of Harold’s Grave and Cliff, respectively (Prichard et al., 1986; Tarkian and Prichard, 1987; Prichard and Tarkian, 1988). These studies used the textural position of PGMs with respect to the silicate host to suggest that Os- and Ru-rich PGM formed before those of Ir-, Pd-, Rh- and, lastly, Pt-bearing PGM. Only Os-rich laurite occurred enclosed by unaltered chromite, with other PGMs either in the altered rim of chromite grains or in interstitial altered silicates, with sperrylite (PtAs_2) found exclusively in the latter textural position. Two distinct platinum-group mineral (PGM) assemblages have been recognized at Harold’s Grave (Badanina et al., 2013a): a ‘primary’ euhedral PGM assemblage, which occurs as inclusions in chromite, and a modified ‘secondary’ subhedral to anhedral PGM assemblage observed in cracks filled by chlorite or serpentine, interstitially to chromite grains. The ‘primary’ PGM assemblage is represented by solitary grains of laurite or Os-rich iridium and composite grains of laurite + Os-rich iridium \pm Ir-rich osmium, whereas the ‘secondary’ PGM assemblage is defined by laurite, Os-rich laurite, irarsite, native osmium and Ru-pentlandite.

Our current study is directed towards identifying the Os-isotope composition of both primary and secondary laurite-alloy assemblages as revealed in individual composite grains enclosed within or interstitially to chromite, respectively, since these are rarely reported from ophiolite deposits (Malitch et al., 2003a, 2014, in press; González-Jiménez et al., 2012b, 2015). We present in-situ Os-isotope compositions of primary and secondary PGM assemblages from Harold’s Grave, along with their PGM chemistry and the whole rock PGE and Os-isotope composition of the host chromitite in order to: 1) compare the isotope signatures of the chromitite, primary and secondary PGM assemblages, and 2) constrain the long-term Re–Os evolution of the Earth’s upper mantle as exemplified by this Late Paleozoic ophiolite complex.

2. Geological background and sample location

The Shetland islands of Unst and Fetlar, lie roughly midway between Norway and the Scottish mainland. The ultramafic and mafic complex

outcropping here was first described as an ophiolite complex by Garson and Plant (1973), an interpretation supported by the majority of subsequent authors (e.g. Flinn et al., 1979; Flinn, 1985; Prichard, 1985). At least two stacked nappes of ophiolitic lithologies are recognized in the Shetland Ophiolite Complex, representing an original structural thickness of 8–10 km (Fig. 1, Flinn, 1985, 2001 and references therein). The variably serpentined protoliths and characteristic stratigraphy of tectonised harzburgite, cumulate dunite, werhlite–pyroxenite layers and isotropic gabbros are recognizable, together

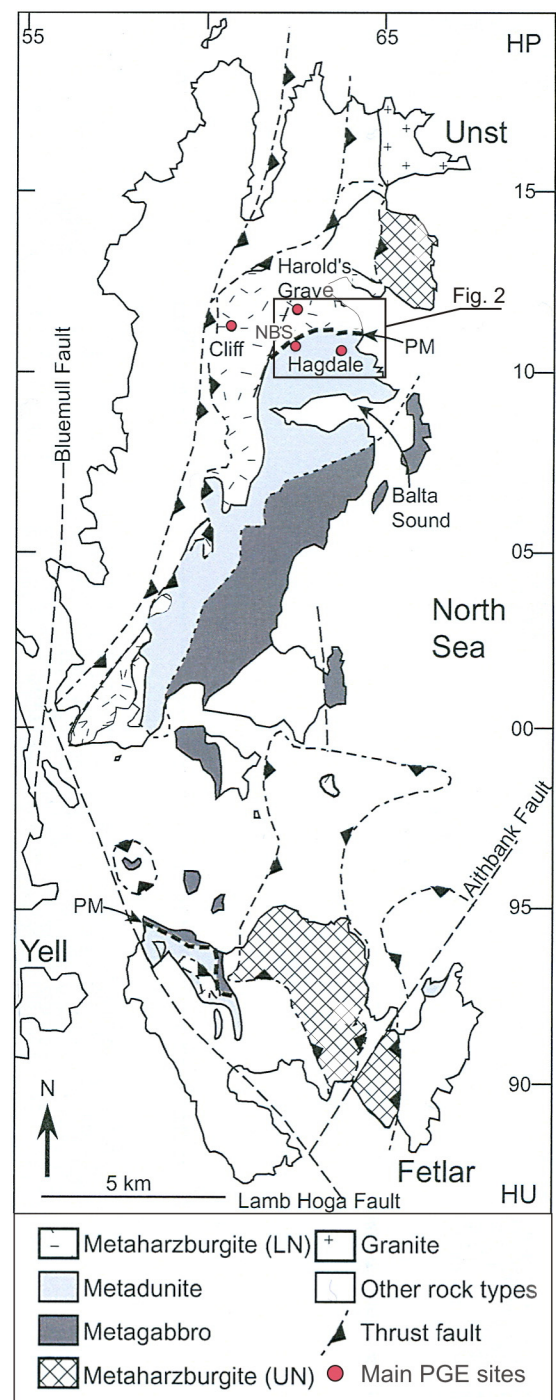


Fig. 1. Simplified geological map of the Isles of Unst and Fetlar, showing major lithological units of the Shetland Ophiolite Complex (after Flinn, 1996, 2001) and location of major PGE-rich chromitite sites at Cliff, Harold’s Grave, North of Baltasound (NSB) and Hagdale including sample RL009 at Harold’s Grave area. The trace of petrological Moho (PM) is also highlighted as are the harzburgites of the upper and lower nappes (UN and LN, respectively). Grid lines are those of the UK National Grid (HP).

with intercalated fragments of a dynamo-metamorphic sole and lower grade metasedimentary rocks (Prichard, 1985). Irregular and isolated podiform chromitite layers, up to 2 m thick, occur in dunite pods or cumulates (Prichard and Lord, 1993).

Crystallization of the SOC is constrained to before 492 ± 3 Ma by the U-Pb age of zircon from a plagiogranite (Spray and Dunning, 1991), with intra-oceanic thrusting, obduction and/or subsequent thrusting constrained to between 479 ± 6 Ma and 465 ± 5 Ma by K-Ar data from hornblende in the metamorphic sole (Spray, 1988). A boninitic dyke swarm cutting gabbros at the uppermost exposed stratigraphic level of the complex indicates a supra-subduction zone setting (Prichard and Lord, 1988), which may provide an explanation for the unusually high concentrations of PGE for an ophiolite complex, in particular for PPGE (Prichard et al., 1996). These are found associated with chromite and weakly disseminated sulphides, located either in dunite pods in harzburgite, or in stratiform discontinuous chromite-rich dunites within the lower crustal sequence above the petrological moho, or with minor sulphide concentrations in pyroxene-rich rocks above, exemplified by the area North of Baltasound (Prichard et al., 1986; Lord, 1991; Lord et al., 1994; Lord and Prichard, 1997; O'Driscoll et al., 2012; Brough et al., 2015). Highly PPGE-enriched chromite-rich lithologies at Cliff have been attributed to subsequent hydrothermal mineralisation during talc-carbonate alteration (Gunn and Styles, 2002) or to localized in situ upgrading of existing magmatic concentrations (Lord et al., 1994). The mineralogy of the Os-, Ir-, Ru- and Rh-bearing PGM from these chromitites and other lithologies have been evaluated elsewhere (Tarkian and Prichard, 1987; Prichard and Tarkian, 1988; Prichard et al., 1986, 1994) including those from Harold's Grave (Prichard et al., 1986; Tarkian and Prichard, 1987; Prichard and Tarkian, 1988; Badanina et al., 2013a). The compositionally heterogenous character of

chromitite occurrences and their late-stage alteration has been reported by Derbyshire et al. (2013) and Brough et al. (2015).

The Harold's Grave locality lies 0.75 km N of the east–west trending petrological Moho and the main concentration of chromite quarries. Although poorly exposed, protolith mapping has shown it is associated with an exceptionally large dunite pod ca. 500 m long (Fig. 2, Lord, 1991), which has been interpreted as evidence of a larger throughput of magma from which to source IPGE (Brough et al., 2015). The textures of the chromite-rich lithologies are particularly massive (Fig. 3), which may be interlayered with serpentinitized dunite. The area is one of the least affected by talc-carbonate alteration of any chromite-rich mantle pod and sufficiently remote to discount any possibility of ore material being transported from other locations, so was selected as ideal for detailed investigation of primary Os isotopes. The material investigated here was from a sub-sample of a single boulder of stockpiled chromitite associated with the trial excavation and was exceptionally large (ca. 10 kg) compared to the ore grade material remaining in the other worked-out locations in the SOC.

3. Analytical techniques

The study combined a number of analytical techniques, including acid digestion and isotope dilution (ID) ICP-MS, electron microprobe analysis and laser-ablation attached to multiple collector inductively coupled plasma mass spectrometry (LA MC-ICP-MS). Whole-rock PGE- and Re-concentrations, and the Os-isotope composition were determined through the application of the high pressure ashing acid digestion and ID-ICP-MS method detailed by Meisel et al. (2001a, 2003) and Paliulionyte et al. (2006). In brief, a test portion of 2 g of fine grained chromitite sample powder was spiked with a mixed PGE and Re

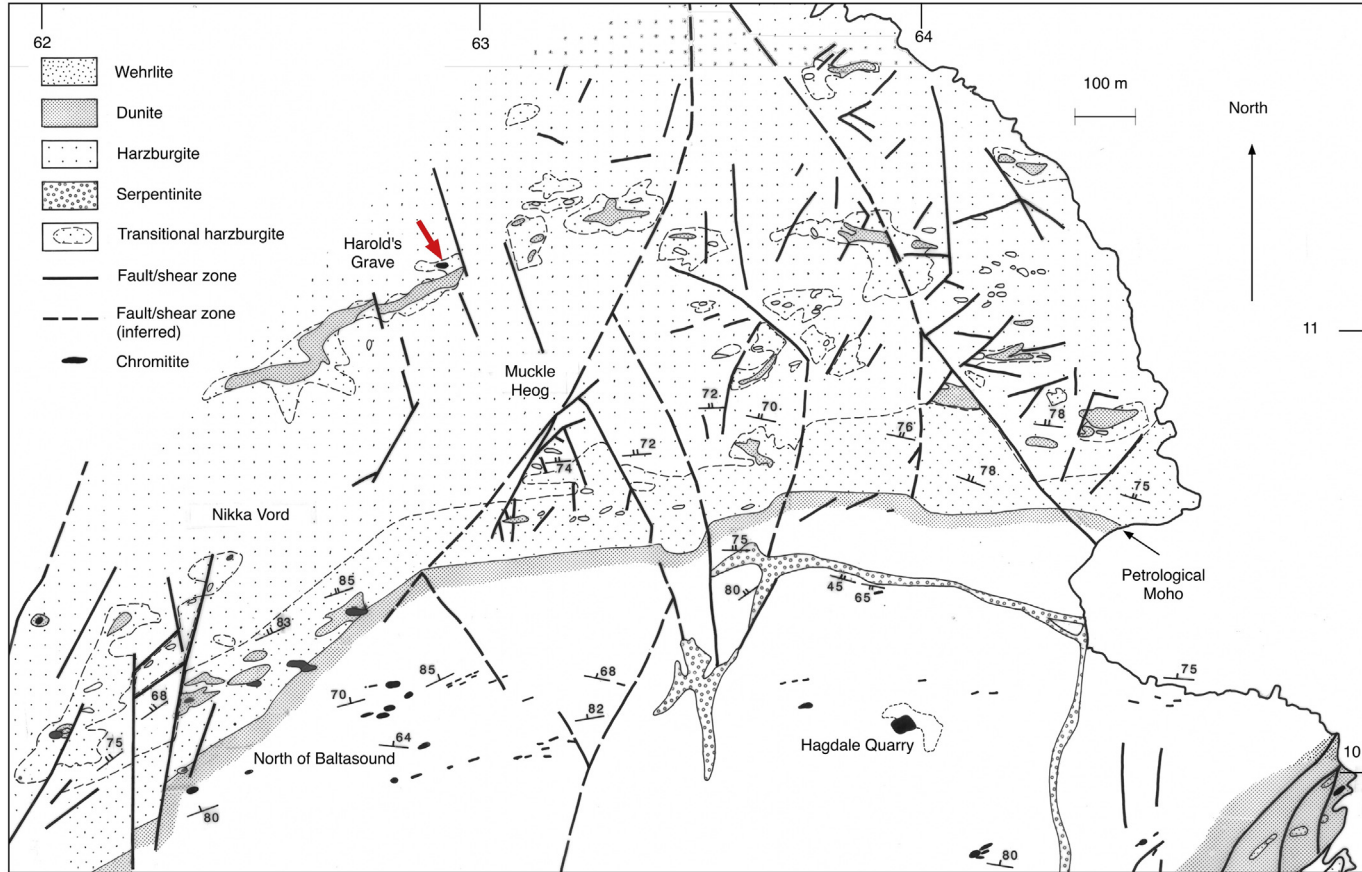


Fig. 2. Geological map of the best-preserved example of the ophiolite stratigraphy in the SOC, showing the relationship of the chromitite quarries at Harold's Grave (red arrow) to dunite pods in the mantle sequence and the major chromitite occurrences North of Baltasound and Hagdale near or above the petrological Moho (after Lord, 1991). (For interpretation of the references to colour in this figure legend, the reader is referred to the web version of this article.)



Fig. 3. Massive texture of chromitite sample RL009 cut for mineralogical and isotopic analysis.

solution, digested in an acid mixture (5 ml of concentrated HNO_3 and 2 ml of concentrated HCl) at 300 °C and 125 bar ($1.25 \times 10^7 \text{ Pa}$) for 10 h in a high pressure asher (HPA-S, Anton Paar, Graz, Austria). The osmium concentration was determined by sparging the OsO_4 that was formed during digestion into the ICP-QMS 7500ce at the General and Analytical Chemistry, Montanuniversität Leoben. The $^{187}\text{Os}/^{188}\text{Os}$ value was calculated after spike and internal mass bias correction. The absolute amount of the analysed inhouse Os reference solution LOsST was equal to two ng of Os. Repeated measurement of the standard solution over a period of two years gave $^{187}\text{Os}/^{188}\text{Os} = 0.1069$ with a standard deviation of less than 1%. The remaining solution was dried down and the Ru, Pd, Re, Ir and Pt concentrations were determined with an online separation procedure as outlined by Meisel et al. (2003). Blanks for Re and Os were always less than 10 pg.

The textural relationships of PGM with the associated gangue minerals were investigated in polished sections using an ARL-SEMQ microprobe equipped with four wavelength-dispersive spectrometers (WDS) and a LINK energy dispersive analyser at the Chair of Resource Mineralogy, Montanuniversität Leoben (Austria). About 2.5 kg of the chromitite sample was disintegrated and milled, followed by sieving and removal of the fine fractions <56 and 56–100 µm. The heavy minerals (including PGMs) within these two fractions were concentrated by a hydroseparation technique (Knauf, 1996; Malitch et al., 2001; Rudashevsky et al., 2002) at NATI Research JSC, St. Petersburg, Russia (<http://www.natires.com>). Each heavy-mineral concentrate was mounted in epoxy blocks and polished in separate sections for further detailed mineralogical and microanalytical studies. About 1060 platinum-group mineral grains have been examined. Microprobe analyses of PGMs were carried out with an ARL-SEMQ microprobe with four WDS and equipped with a LINK energy dispersive analyser (Montanuniversität Leoben) and a CAMECA SX-100 equipped with five WDS spectrometers and a Bruker energy dispersive spectrometer system (Institute of Geology and Geochemistry, UB RAS). Details of the analytical procedures are described by Malitch et al. (2001) and Badanina et al. (2013b).

The main set of LA measurements was performed with a Microprobe II LA device (Thermo Elemental, Nd:YAG laser, 266 nm wavelength) and an AXIOM MC-ICPMS (Thermo Elemental Axiom, multicollector version featuring 9 Faraday cup detectors operated at a mass resolution of 400) at the Technical University of Mining and Metallurgy, Freiberg, Germany. The ICP-MS was tuned using a desolvating nebulizer (MCN 6000, CETAC), a solution of 33 µg/l Re, 330 µg/l Os, and 330 µg/l Ir in 2% nitric acid, a nebulizer flow of 0.8 l/min Ar, and a radio frequency (RF) forward power of 1330 W. Helium was used as an ablation chamber gas with a flow of 85 ml/min that has minimized dead volume. The air capacitor of the ICP-MS was optimized to obtain a RF reflected power

of 12 to 18 W with this He addition to the plasma gas. The MC set-up, and corrections for Re and W contents, were checked with combined laser ablation analyses of members of the hubnerite (MnWO_4) – ferberite (FeWO_4) series and the aerosol generated by the desolvating nebulizer, as described by Junk (2001). LA spots of 15 to 30 µm were used with a scan field that was adapted to the size of each sampling area (Figs. 4 and 5), a laser shot frequency of 20 Hz, and an energy output of up to 0.5 mJ. The aerosols generated by LA were transported by a gas stream to the MC-ICP-MS. Nine signals were measured simultaneously at m/z 183 (W), 184 (W + Os), 185 (Re), 186 (W + Os), 187 (Re + Os), 188 (Os), 189 (Os), 191 (Ir) and 193 (Ir) using the multi-channel collector of the ICP-MS. The mass bias was corrected using an exponential fractionation law and the $^{188}\text{Os}/^{189}\text{Os}$ ratio. All the analysed grains have $^{187}\text{Re}/^{188}\text{Os}$ lower than 0.005, thus ensuring that the isobaric interference of ^{187}Re on ^{187}Os was precisely corrected (cf. Nowell et al., 2008). The abundances used for the calculations were taken from Rosman and Taylor (1998) (at.%, $^{184}\text{Os} = 0.02$, $^{186}\text{Os} = 1.59$, $^{188}\text{Os} = 13.24$, $^{189}\text{Os} = 16.15$, $^{190}\text{Os} = 26.26$ and $^{192}\text{Os} = 40.78$). The isotope ratios are reported with experimental uncertainties taking into account the contributions of the Faraday cup efficiencies, the normalization value for mass bias corrections using $^{188}\text{Os}/^{189}\text{Os}$ (Rosman and Taylor, 1998), interference corrections, the signal noise, and the within-run standard deviations. Repeated analyses ($n = 36$) of a natural Os-Ir alloy, which has been used to check the validity of the LA MC-ICP-MS measurements, yield $^{187}\text{Os}/^{188}\text{Os} = 0.12166 \pm 0.00018$ (2 sigma uncertainty). Furthermore, it has been shown (Malitch et al., 2002) that the Os isotopic composition of Os-Ir alloy (i.e., $\text{Os}_{0.89}\text{Ir}_{0.11}$) from the Bor-Uryah massif measured by LA MC-ICP-MS ($^{187}\text{Os}/^{188}\text{Os} = 0.12396 \pm 0.00013$) is in accordance with N-TIMS analysis of the same sample ($^{187}\text{Os}/^{188}\text{Os} = 0.1240 \pm 0.0002$). A more detailed description of the LA MC-ICP-MS technique is given by Junk (2001). In addition, 11 in-situ Os isotope analyses were carried out at Geochemical Analysis Unit at the GEMOC laboratories (Macquarie University, Sydney, Australia, ESM Appendix 1) using analytical methods described in detail by Pearson et al. (2002), Marchesi et al. (2011) and González-Jiménez et al. (2015). These analyses used a Nu Plasma Multicollector ICP-MS attached to a New Wave/Merchantek UP 213 laser microprobe. Ablation was carried out with a frequency of 4 Hz, energies of 1–2 mJ/pulse and a spot size ranging from 15 to 30 µm. A standard NiS bead (PGE-A) with 199 ppm Os (Lorand and Alard, 2001) and $^{187}\text{Os}/^{188}\text{Os} = 0.1064$ (Pearson et al., 2002) was analysed between PGM samples to monitor any drift in the Faraday cups. These variations were typically less than 0.2% over an analytical session. The data were collected using the Nu Plasma time-resolved software, which allows the selection of the most stable intervals of the signal for integration. The selected interval was divided into 40 replicates to provide a measure of the standard error. Under the ablation conditions described above, given the analysed grains had average sizes >100 µm and Os average contents of ~5 wt.%, a typical run duration of ~100 s was achieved with an average signal intensity of Os ~ 1.9 V on the Faraday cups. This gives a precision for $^{187}\text{Os}/^{188}\text{Os}$ ranging from 4.0×10^{-5} to 10.0×10^{-5} (SE). The accuracy of the data presented here is similar to that of Os-Ir alloys from chromitites in the Luobusa (Tibet) Ophiolite as illustrated by independent data sets (different instruments, operating protocols); Shi et al. (2007) reported a mean $^{187}\text{Os}/^{188}\text{Os} = 0.12646 \pm 11$ (1SE, $n = 148$) while Pearson et al. (2007) reported $^{187}\text{Os}/^{188}\text{Os} = 0.12653 \pm 7$ (1SE, $n = 80$). The quoted uncertainties on T_{MA} and T_{RD} model ages include the uncertainties in the measured $^{187}\text{Os}/^{188}\text{Os}$ and $^{187}\text{Re}/^{188}\text{Os}$, calculated according to the equation of Cambridge and Lambert (1997).

4. Results

4.1. PGE concentrations and Os-isotope data in chromitite

The total PGE concentrations in the chromitite sample studied are typical of those reported for Harold's Grave (Table 1) and at ΣPGE of

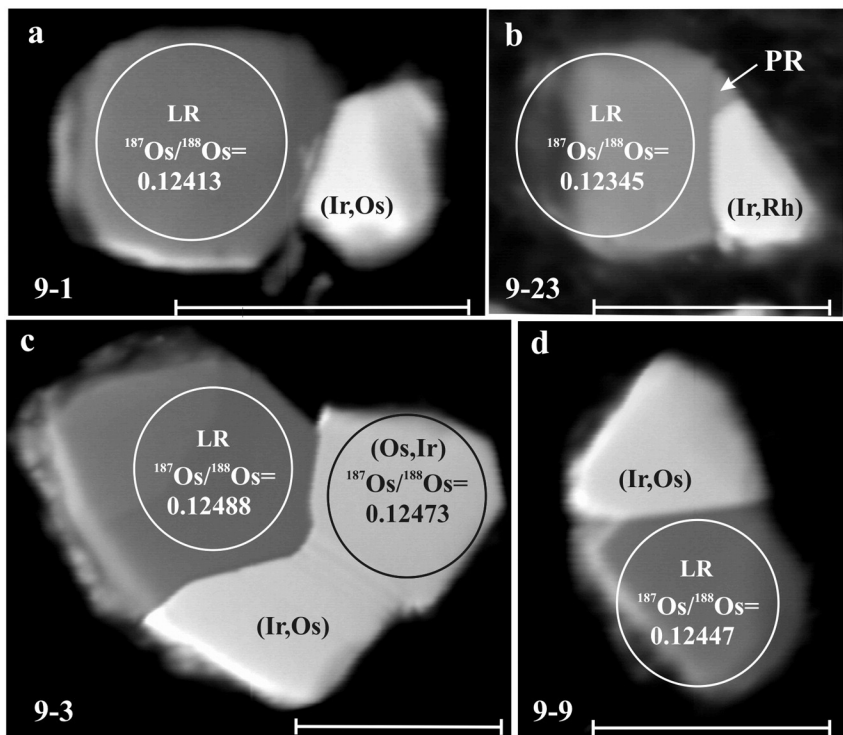


Fig. 4. Back scattered electron images of euhedral composite PGM grains from podiform chromitite at Harold's Grave. LR – laurite; (Ir,Os) – Os-rich iridium; (Os,Ir) – Ir-rich osmium. Circles denote areas of laser ablation MC-ICP-MS analyses; $^{187}\text{Os}/^{188}\text{Os}$ values correspond to those in Table 4. Scale bar is 30 microns.

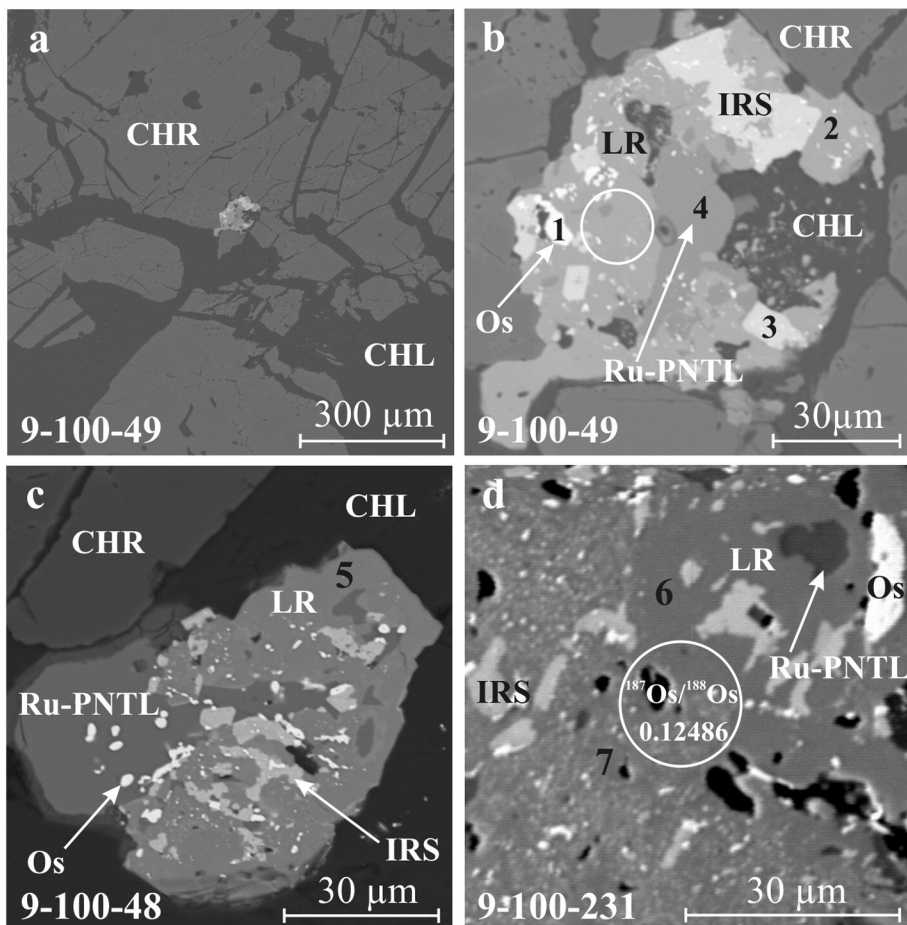


Fig. 5. Back scattered electron images of secondary PGM assemblages in chromitite at Harold's Grave. LR – laurite; Os – osmium; IRS – irarsite; Ru-PNTL – Ru-bearing pentlandite; CHR – chromite; CHL – chlorite; numbers 1-7 denote areas of electron microprobe analyses corresponding to the same numbers in Table 3. Circles denote areas of laser ablation MC-ICP-MS analyses.

Table 1

Concentrations of PGE, Au, Re (all in ppb) and Os-isotopic signature of chromitites from Harold's Grave.

Sample ID	Lithology	Os	Ir	Ru	Rh	Pt	Pd	Au	Re	$^{187}\text{Os}/^{188}\text{Os} \pm 2\sigma$	ΣPGE	$\Sigma\text{IPGE}/\Sigma\text{PPGE}$	Source
Cr.	Chromitite	–	1803	4014	249	325	20	–	–	–	6411	9.79	Gunn et al. (1985)
Cr.	Chromitite	–	831	740	129	250	19	–	–	–	1969	3.95	Gunn et al. (1985)
F	Chromitite	800	1100	1800	220	370	3400	–	–	–	7690	0.93	Prichard et al. (1986)
G	Chromitite	302	298	527	107	100	<8	–	–	–	1334	5.44	Prichard et al. (1986)
RL069	Dunite host to RL070	170	180	320	57	170	24	<2	–	–	921	2.67	Lord (1991)
RL070	Chromitite layer	520	550	960	140	330	56	<2	–	–	2556	3.86	Lord (1991)
3	Chromitite	729	–	–	–	–	–	0.9237	$0.12523 \pm <0.000125$	–	–	–	Walker et al. (2002b)
HG1	Chromitite	701	546	2356	–	459	112	–	0.0161	0.125542 ± 0.000042	4174	6.31	O'Driscoll et al. (2012)
HG2	Chromitite	1693	1485	3440	–	1220	121	–	0.1223	0.124896 ± 0.000001	7959	4.94	O'Driscoll et al. (2012)
HG2 Rep	Chromitite	997	667	3000	–	846	65	–	0.1168	0.125298 ± 0.000001	5575	5.12	O'Driscoll et al. (2012)
HG3	Chromitite	1117	1012	2999	–	1124	122	–	0.0473	0.125229 ± 0.000006	6374	4.12	O'Driscoll et al. (2012)
RL009	Chromitite	2302	1197	4517	214	333	24	–	–	–	8587	14.04	Badanina et al. (2013a)
HG11	Chromitite	2012	2127	3533	345	504	41	–	–	–	8562	8.62	Brough et al. (2015)
HG5	Chromitite	1067	2073	2964	306	428	38	–	–	–	6876	7.91	Brough et al. (2015)
HG7	Chromitite	1324	2270	3483	397	785	69	–	–	–	8328	5.66	Brough et al. (2015)
HG1	Chromitite	1647	2040	3400	349	474	40	–	–	–	7950	8.21	Brough et al. (2015)
HG1 rep	Chromitite	1587	1901	3252	331	431	42	–	–	–	7544	8.38	Brough et al. (2015)
HG8	Chromitite	1479	2088	3183	344	685	36	–	–	–	7815	6.34	Brough et al. (2015)
HG9	Chromitite	650	1159	2172	257	480	53	–	–	–	4771	5.04	Brough et al. (2015)
HG4	Chromitite	1325	1974	3069	336	463	54	–	–	–	7221	7.47	Brough et al. (2015)
HG6	Chromitite	2968	2861	7311	422	566	40	–	–	–	14,168	12.78	Brough et al. (2015)
RL009	Chromitite	2302	1197	4517	214	333	24	–	0.42	0.1240 ± 0.0006	8587	14.04	Badanina et al. (2013a, this study)

8587 ppb are very high compared to typical ophiolitic chromitite, for which total PGE is commonly <500 ppb (Melcher, 2000). Consistently high whole-rock PGE concentrations in chromitites from Harold's Grave give negatively sloped chondrite-normalized PGE patterns (Fig. 6), typical of many mantle hosted 'ophiolitic' chromitites, in which IPGE prevail over PPGE. The $^{187}\text{Os}/^{188}\text{Os}$ value of the chromitite at Harold's Grave in this study (0.1240 ± 0.0006) is slightly less radiogenic than that of chromitite samples from the same locality (0.12489 – 0.12554) presented by Walker et al. (2002b) and O'Driscoll et al. (2012).

4.2. Primary and secondary PGM assemblages at Harold's Grave

Following an extensive survey of 1060 PGM grains, two contrasting PGM assemblages have been shown to occur at Harold's Grave, even within the same chromitite block (Table 2). These are distinguished by their differing morphology and internal texture (Figs. 4 and 5). Firstly, euhedral PGM (up to 55 μm in size) occur as inclusions within chromite,

indicating this is a "primary" magmatic assemblage; secondly, subeuhedral to anhedral PGM (up to 500 μm) occur in association with pentlandite in serpentine- or chlorite-filled cracks or interstitially to chromite grains, indicating a "secondary" modified assemblage. The primary PGM assemblage is represented by 156 solitary grains of laurite and/or Os-rich iridium, or by polyphase groups of grains that display regular phase boundaries between two or three distinct PGMs (Table 2, Fig. 4). The latter are predominately laurite \pm Os-rich iridium (Fig. 4a, d), with subordinate examples of laurite + Os-rich iridium + Ir-rich osmium (Fig. 4c) and more rarely laurite + Ir-Rh alloy + Rh-rich sulphide, possibly prassoite (Fig. 4b). In contrast, the 'secondary' PGM assemblage is represented by 904 grains, which are polyphase, complex and irregular. Again laurite is dominant, but now intimately intergrown with Os-bearing laurite, native osmium, irarsite and Ru-rich pentlandite (Table 2, Fig. 5). Other secondary PGM examples include the irarsite-hollingworthite series (IrAsS–RhAsS), tololvite (IrSbS), geversite (PtSb₂) and Ru-rich oxide, which occur in subordinate amounts (Table 2).

Table 3 gives representative analyses of PGMs that constitute secondary polyphase grains in Fig. 5, whereas Fig. 7 shows the chemical variation of laurite and Os-rich alloys encountered. More detailed compositional characteristics of the primary PGM assemblage have been presented in Badanina et al. (2013a).

4.3. In-situ Os-isotope data

'Primary' solitary laurite grains and polyphase laurite-alloy pairs preserved in the chromite cores have $^{187}\text{Os}/^{188}\text{Os}$ values between 0.1214 and 0.1252, with a mean of 0.1242 ± 0.0008 (2 sigma, n = 25), and $^{187}\text{Re}/^{188}\text{Os}$ mainly lower than 0.0003 (Tables 4 and 5). The 'secondary' PGM assemblage is characterized by a similar degree of Os-isotope variations, but with a slightly higher resulting value ($^{187}\text{Os}/^{188}\text{Os}$ values range from 0.1234 to 0.1276 with a mean of 0.1245 and a standard deviation of 0.0006, n = 69, ESM Appendix 1, Table 5). In our data set only two analyses of primary PGM (samples 9–19 and 9–29–1, Table 4) showed less radiogenic Os-isotope values, whereas only two analyses of secondary PGMs (samples 9–100–20 and 9–100–97) deviate from the mean towards more radiogenic Os-isotope values (Tables 4 and 5; ESM Appendix 1; Fig. 8). The osmium

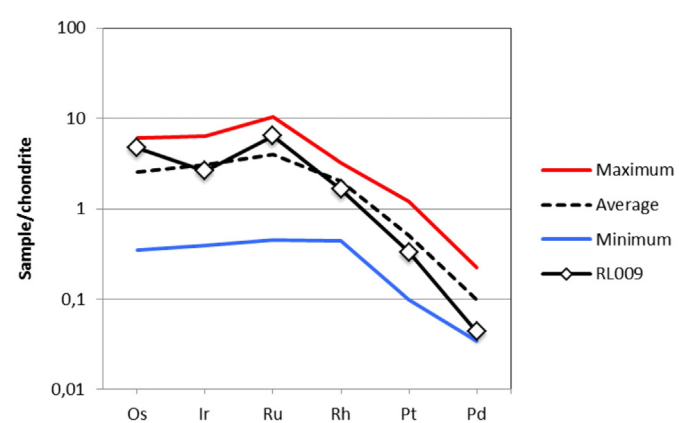


Fig. 6. Chondrite-normalised PGE patterns of podiform chromitites at Harold's Grave (Shetland ophiolite complex). Composition of chondrite according to McDonough and Sun (1995).

Table 2

PGM assemblages at the Harold's Grave chromitite occurrence.

	Primary assemblage (this study, Badanina et al., 2013a)	Secondary assemblage (this study)	Additional minerals reported in other studies ^{1,2}
Dominant Os-, Ir-, Ru-bearing, IPGE minerals and associations ³	Solitary grains of: Os-rich iridium (Ir,Os), or laurite (RuS_2) Composite grains: mainly laurite + Os-rich iridium, lesser laurite + Os-rich iridium + Ir-rich osmium (Os,Ir)	Laurite, Os-rich laurite, Irarsite (IrAsS), Native osmium, Ru-pentlandite	
Rare phases, including Rh–Pt–Pd-bearing, IPGE minerals)	Ir–Rh alloy + Rh-rich sulphide (prassoite?) as composite grains with laurite)	Irarsite-hollingworthite ss series ($\text{IrAsS}-\text{RhAsS}$), Tolovkite (IrSbS), Geversite (PtSb_2), Ru-rich oxide	Genkinite $((\text{Pt},\text{Pd})_4\text{Sb}_3)^1$, hongshiite (PtCu^1), Pt–Pd–Cu alloy ¹ mertieite I/II or stibiopaladinite $((\text{Pd},\text{Cu})_{5-11}(\text{Sb},\text{As})_{2-4})^1$ Rh, Sb, S ¹ Rh, Ni, Sb ¹
Texture (shape)	Euhedral, regular internal phase boundaries	Subhedral to anhedral, complex, irregular, intimately intergrown	
Texture (position)	Inclusions enclosed by chromite	In chlorite or serpentine, in cracks within or interstitially to chromite	
Size μm	<55 μm	<500 μm	Laurite up to <400 μm ²
Number of grains	156	904	

¹ Prichard and Tarkian (1988).² Prichard et al. (1994).³ Note that laurite commonly contains Ir and Rh as well as Os, whereas Os-rich iridium contains Rh and Pt, and Ir-rich osmium contains Rh, see Badanina et al. (2013a) for details.

isotope results identify a restricted range of broadly similar $^{187}\text{Os}/^{188}\text{Os}$ values for 'primary' and 'secondary' PGM assemblages (Fig. 8, Table 5). Similarly, both model Os-ages (i.e., T_{MA} and T_{RD}) of primary and secondary PGMs, calculated relative to an Enstatite Chondrite Reservoir (ECR) model (Walker et al., 2002a; Shi et al., 2007), are characterized by similar age clusters (550 ± 111 Ma and 508 ± 85 Ma, respectively, Table 5).

5. Discussion

5.1. Compositional and experimental constraints on genesis of polyphase PGM assemblages

Platinum-group minerals are commonly hosted by podiform chromitites within residual mantle and banded chromitites located in

Table 3

Selected electron microprobe (WDS) analyses of minerals from secondary PGM assemblage at Harold's Grave.

Analysis	1	2	3	4	5	6	7
Sample	9–100–49	9–100–49	9–100–49	9–100–49	9–100–48	9–100–231	9–100–231
Figure	5b	5b	5b	5b	5c	5d	5d
Mineral	Osmium	Laurite	Irarsite	Ru-PNTL	Laurite	Laurite	Laurite
wt.%							
S	0.00	37.05	11.36	30.41	38.26	37.89	36.59
As	0.00	0.00	26.11	0.00	0.00	0.00	0.00
Sb	0.00	0.00	0.00	0.00	0.00	0.00	0.00
Fe	0.00	0.00	0.00	21.82	0.00	0.00	0.00
Ni	0.00	0.00	0.00	34.63	0.00	0.00	0.00
Cu	0.00	0.00	0.00	0.00	0.00	0.00	0.00
Ru	0.87	53.56	3.14	12.22	57.28	56.23	52.42
Rh	0.00	0.00	4.54	0.00	0.00	0.00	0.00
Os	93.19	7.02	3.32	0.00	3.08	2.86	5.61
Ir	5.90	1.78	51.58	0.00	1.35	3.23	5.14
Pt	0.00	0.00	0.00	0.00	0.00	0.00	0.00
Total	99.96	99.41	100.05	99.08	99.97	100.21	99.76
at.%							
S	0.00	66.73	33.31	46.27	66.92	66.77	66.50
As	0.00	0.00	32.76	0.00	0.00	0.00	0.00
Sb	0.00	0.00	0.00	0.00	0.00	0.00	0.00
Fe	0.00	0.00	0.00	19.06	0.00	0.00	0.00
Ni	0.00	0.00	0.00	28.78	0.00	0.00	0.00
Cu	0.00	0.00	0.00	0.00	0.00	0.00	0.00
Ru	1.63	30.60	2.92	5.90	31.78	31.43	30.22
Rh	0.00	0.00	4.15	0.00	0.00	0.00	0.00
Os	92.57	2.13	1.64	0.00	0.91	0.85	1.72
Ir	5.80	0.53	25.22	0.00	0.39	0.95	1.56
Pt	0.00	0.00	0.00	0.00	0.00	0.00	0.00
Ru number		93			97	97	95

Note. Analysis numbers refer to points on Fig. 5. Abbreviations: Ru-PNTL – Ru-bearing pentlandite; Ru number of laurite equals to $100 \times \text{Ru}_{\text{at.\%}} / (\text{Ru} + \text{Os})_{\text{at.\%}}$.

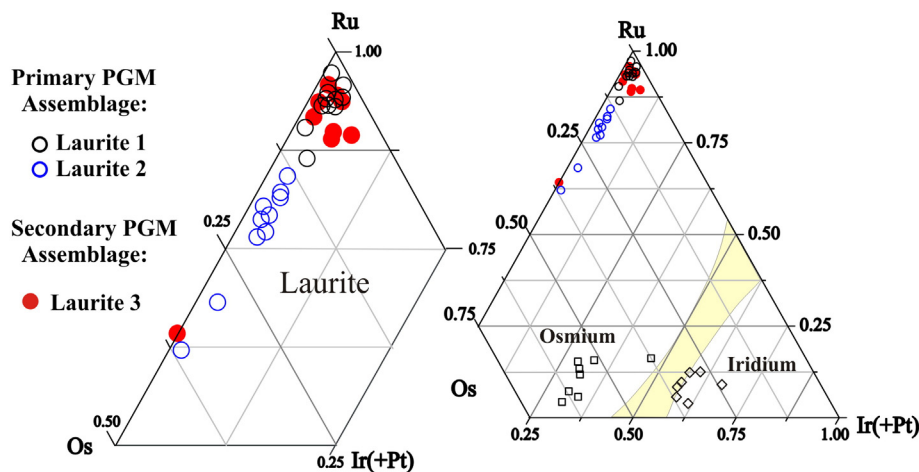


Fig. 7. Composition of laurite (a and b) and Os-rich alloys (b) from podiform chromitite at Harold's Grave in the ternary diagrams Ru-Os-Ir, at %. Symbols: open circles, laurite; open squares, Ir-rich osmium and open diamonds, Os-rich iridium. In 7b, yellow area corresponds to miscibility gap between osmium and iridium (Harris and Cabri, 1991). (For interpretation of the references to colour in this figure legend, the reader is referred to the web version of this article.)

either the transition zone or crustal section of an ophiolite complex. Both types of chromitite are generally well defined based on distinct geological, geochemical and mineralogical features (Lago et al., 1982; Dick and Bullen, 1984; Augé and Johan, 1988; Leblanc, 1991; Melcher, 2000; Malitch et al., 2003b; Prichard et al., 2008; González-Jiménez et al., 2010; Akmaz et al., 2014, among many others).

Reports of contrasting PGM assemblages within a particular chromitite pod are rare (Prichard and Tarkian, 1988; Malitch et al., 2001; Badanina et al., 2013a; González-Jiménez et al., 2015). Studies of the Kraubath ophiolite, Austria (Malitch et al., 2003b) and the Guli complex, Russia (Malitch et al., 2002) have shown similar primary PGM assemblages (e.g., laurite, Os-rich iridium and Ir-rich osmium). Elsewhere, laurite is intimately intergrown with either Os-rich iridium, as in the Tiebagi ophiolite, New Caledonia (Augé, 1988), the Samar ophiolite, Philippines (Nakagawa and Franco, 1997), or with Ir-rich osmium, as seen in the Vourinos ophiolite, Greece (Augé, 1985), the Thetford ophiolite, Canada (Corrivaux and Laflamme, 1990) and the

Samar ophiolite, Philippines (Nakagawa and Franco, 1997). Complex PGM assemblages (those composed of variety of S- and As-bearing PGM) are thought to indicate chromitites formed in the upper mantle under exceptionally high fluid activity (Torres-Ruiz et al., 1996; Melcher et al., 1997; Garuti et al., 1999).

Recent experimental data (Brenan and Andrews, 2001; Andrews and Brenan, 2002) evaluated quantitatively the effects of T and $f(S_2)$ for laurite + alloy mineral pairs. The compositional results of associated laurite and Os-rich alloys at Harold's Grave (Badanina et al., 2013a) fit the predicted compositions of experiment W-1200-0.37 that produced laurite and two compositionally distinct alloys (e.g. Ir-rich osmium and Os-rich iridium, both with approximately equal Ru contents, Fig. 3c in Andrews and Brenan, 2002). The analogy with these high temperature experiments (at 1200–1250 °C) indicates that the natural laurite–alloy pairs observed were trapped as primary magmatic phases with an ambient $f(S_2)$ in the range of $10^{-0.39}$ to $10^{-0.07}$ atm (Andrews and Brenan, 2002). The polyphase character of the primary PGM

Table 4

Os isotope composition, model T_{Ma} and T_{RD} ages of platinum-group minerals from primary PGM assemblage at Harold's Grave.

Sample, figure	PGM assemblage	^{188}Os	$^{187}\text{Os}/^{188}\text{Os}$	Uncertainty (1σ)	$^{187}\text{Re}/^{188}\text{Os}$	$^{187}\text{Os}/^{188}\text{Os(i)}$	γOs	T_{Ma} (Ga)	1σ (Ga)	T_{RD} (Ga)	1σ (Ga)
9-1_Fig. 4a	LR + (Ir,Os)	0.28	0.12413	0.00009	0.0001	0.1241	-3.10	0.564	0.010	0.563	0.010
9-2	LR + (Ir,Os)	0.25	0.12402	0.00007	0.0001	0.1240	-3.19	0.579	0.013	0.579	0.013
9-3-1_Fig. 4c	LR + (Os,Ir) + (Ir,Os)	0.29	0.12488	0.00006	0.0001	0.1249	-2.49	0.453	0.008	0.453	0.008
9-3-2_Fig. 4c	LR + (Os,Ir) + (Ir,Os)	0.22	0.12473	0.00009	0.0002	0.1247	-2.63	0.479	0.013	0.479	0.013
9-9_Fig. 4d	LR + (Ir,Os)	0.25	0.12447	0.00006	0.0001	0.1245	-2.83	0.515	0.008	0.515	0.008
9-15	LR	0.34	0.12508	0.00009	0.0001	0.1251	-2.36	0.429	0.013	0.429	0.013
9-19	Os-LR	0.23	0.12137	0.00007	0.0002	0.1214	-5.25	0.952	0.010	0.952	0.010
9-20	LR	0.12	0.12447	0.00009	0.0001	0.1245	-2.83	0.515	0.013	0.515	0.013
9-23_Fig. 4b	LR + (Ir,Os) + PR	0.09	0.12345	0.00011	0.0001	0.1234	-3.64	0.661	0.016	0.661	0.016
9-28	LR + (Ir,Os)	0.42	0.12520	0.00004	0.0001	0.1252	-2.26	0.412	0.006	0.412	0.006
9-29-1	LR + (Ir,Os)	0.18	0.12325	0.00016	0.0001	0.1233	-3.79	0.688	0.023	0.687	0.023
9-29-2	LR	0.23	0.12363	0.00009	0.0003	0.1236	-3.49	0.634	0.013	0.634	0.013
9-161	(Os,Ir) + (Ir,Os)	0.07	0.12407	0.00033	0.0003	0.1241	-3.15	0.572	0.047	0.572	0.047
9-146	LR + (Ir,Os)	0.44	0.12433	0.00005	0.0002	0.1243	-2.94	0.535	0.007	0.535	0.007
9-134	LR	0.23	0.12449	0.00007	0.0002	0.1245	-2.82	0.513	0.010	0.512	0.010
9-133	(Ir,Os,Ru)	0.15	0.12354	0.00015	0.0005	0.1235	-3.56	0.647	0.021	0.647	0.021
9-102	LR	0.86	0.12464	0.00003	0.0004	0.1246	-2.70	0.492	0.004	0.491	0.004
9-101	LR	0.46	0.12475	0.00005	0.0001	0.1248	-2.62	0.476	0.007	0.476	0.007
9-78	LR	0.13	0.12391	0.00009	0.0002	0.1239	-3.27	0.595	0.013	0.594	0.013
9-76	(Ir,Os)	0.33	0.12459	0.00010	0.0004	0.1246	-2.74	0.499	0.014	0.498	0.014
9-61	(Ir,Os)	0.12	0.12425	0.00009	0.0004	0.1243	-3.01	0.547	0.013	0.546	0.013
9-38	LR + (Ir,Os)	0.14	0.12491	0.00008	0.0001	0.1249	-2.49	0.453	0.011	0.453	0.011
9-37	LR + (Ir,Os)	0.30	0.12479	0.00006	0.0001	0.1248	-2.58	0.470	0.008	0.470	0.008
9-36	LR	0.44	0.12415	0.00010	0.0006	0.1242	-3.08	0.561	0.014	0.561	0.014
9-35	LR	0.28	0.12441	0.00007	0.0004	0.1244	-2.88	0.524	0.010	0.524	0.010
Average (n = 25)						0.1242		0.550		0.550	

LR – laurite, Os-LR – Os-bearing laurite, (Os,Ir) – osmium, (Ir,Os) and (Ir,Os,Ru) – iridium, PR – prassoite, T_{Ma} and T_{RD} ages were calculated with ECR values estimated by Walker et al. (2002a) and a decay constant of $\lambda = 1.666 \times 10^{-11} \text{ year}^{-1}$ (Smoliar et al., 1996). Uncertainties on model ages are based on within run errors only.

Table 5

Summary of Os-isotope data for primary and secondary PGM assemblages from ophiolite complexes.

Massif	PGM assemblage	$^{187}\text{Os}/^{188}\text{Os}$				$^{187}\text{Re}/^{188}\text{Os}$				$T_{\text{MA}} = T_{\text{RD}}$ (Ma)			
		Mean	Min	Max	Sd	Mean	Min	Max	Sd	Mean	Min	Max	Sd
Shetland	Primary (n = 25)	0.12422	0.12137	0.12520	0.00079	0.00022	0.0001	0.0006	0.00015	550	412	952	111
	Secondary (n = 69)	0.12452	0.12344	0.12763	0.00060	0.00028	0.0001	0.0024	0.00039	508	67	661	85
	Primary and secondary (n = 94)	0.12444	0.12137	0.12763	0.00066	0.00026	0.0001	0.0024	0.00034	519	67	952	94
Nurali ^a	Primary (n = 26)	0.12515	0.12486	0.12553	0.00020	0.00006	0.00001	0.00061	0.00012	420	365	461	29
	Secondary (n = 34)	0.12520	0.12474	0.12568	0.00022	0.00008	0.00001	0.00046	0.00011	412	344	478	32
	Primary and secondary (n = 60)	0.12518	0.12474	0.12568	0.00021	0.00007	0.00001	0.00061	0.00011	415	344	4780	31

Sd — standard deviation.

^a After Malitch et al. (2015).

assemblage at Harold's Grave argues against an origin of these PGM by subsolidus exsolution from the chromite host, rather as earlier crystals enclosed by chromite. The origin of the secondary PGM assemblage has been discussed previously (Tarkian and Prichard, 1987; Prichard and Tarkian, 1988 among others) and is considered to reflect processes such as in-situ sub-oceanic serpentinitisation, alteration during emplacement and/or post-emplacement regional greenschist metamorphism.

5.2. Constraints on Os-isotope variability in platinum-group minerals

The early formation of laurite and Os-Ir alloys at high temperatures implies that the original Os-isotope composition of these PGMs reflects the source region in the mantle at the time of formation. Therefore, the low and similar $^{187}\text{Os}/^{188}\text{Os}$ values in laurite and Os-Ir alloys clearly indicate a common near-chondritic mantle source for the PGE. The osmium isotope results of this study display a restricted range of 'unradiogenic' $^{187}\text{Os}/^{188}\text{Os}$ values for intimately intergrown laurite and Os-rich alloy pairs that form a 'primary' PGM assemblage enclosed by chromite (0.12473–0.12488, Fig. 4c). In such pairs the Os isotope signature of the adjacent phases are indistinguishable. Furthermore, this study shows similar 'unradiogenic' $^{187}\text{Os}/^{188}\text{Os}$ values for both primary and secondary PGM assemblages (with a weighted mean of 0.1242 ± 0.0008 and 0.1245 ± 0.0006 , respectively, Tables 4, 5 and ESM Appendix 1; Fig. 8) that are also consistent (within uncertainty) with the 'unradiogenic' $^{187}\text{Os}/^{188}\text{Os}$ value found for the bulk chromitite (0.1240 ± 0.0006). Our Os-isotope compositions are slightly less radiogenic than those of chromitite samples from the same locality previously reported by Walker et al. (2002b) and O'Driscoll et al. (2012) (e.g., 0.12489–0.12554, Table 1). A similarly restricted range of $^{187}\text{Os}/^{188}\text{Os}$ values has been identified in primary and secondary PGM assemblages (with weighted mean $^{187}\text{Os}/^{188}\text{Os}$ of 0.12515 ± 0.00020 and 0.12520 ± 0.00022 , respectively) from a metamorphosed

chromitite of the Nurali lherzolite-gabbro massif, South Urals (Table 5, Malitch et al., in press). At Nurali, the primary Ru-Os sulphides are commonly replaced by a secondary unnamed Ru-Os-Fe-Ir oxide, providing evidence for various stages of desulfurization and oxidation of primary laurite (e.g., with or without laurite relics). As is the case at Harold's Grave, the Os isotope mineral compositions closely match the whole rock Os isotope signature ($^{187}\text{Os}/^{188}\text{Os} = 0.1254 \pm 0.0002$; Tessalina et al., 2007). Since the PGMs from the secondary assemblage show evidence for alteration, it is possible that their initial $^{187}\text{Os}/^{188}\text{Os}$ could have been modified by reaction with post-magmatic hydrothermal fluids as proposed by González-Jiménez et al. (2012b). The absence of radiogenic $^{187}\text{Os}/^{188}\text{Os}$ values in secondary PGMs, however, suggests that crustal-derived hydrothermal fluids were not supplying radiogenic ^{187}Os . The Os isotope results at Shetland and Nurali are in sharp contrast with the distinctly different Os isotope compositions observed in primary and secondary PGMs from the metamorphosed chromitites of the Dobromirtsi ophiolite massif, Bulgaria (González-Jiménez et al., 2012b), where the larger range in $^{187}\text{Os}/^{188}\text{Os}$ within the secondary PGMs has been attributed to the interaction of the primary PGMs with a metamorphic-hydrothermal fluid, pointing to open-system behaviour of the Re-Os system in PGMs during metamorphism.

The Os-isotope similarity of PGM assemblages and chromitite at Harold's Grave (Tables 1 and 5; Fig. 8) and Nurali (Table 5; Tessalina et al., 2007) implies that the whole-rock Os isotope budget is largely controlled by the observed PGM assemblages and possibly by base metal sulphides of similar Os-isotope composition. The observed Os-isotope similarity of PGM assemblages also supports the conclusion that the secondary PGMs have preserved the subchondritic osmium isotope signature of the primary PGMs during alteration, showing no evidence for other crustal source contributions (e.g., suprachondritic material) during later thermal events. Therefore, Os-isotope data documented at Shetland (this study) and Nurali (Malitch et al., 2014, in press) are consistent with a closed-system behaviour of the Re-Os isotope system in primary and secondary PGMs, preserving mantle signatures during crustal alteration processes. A high resistance of the Os isotope system within PGMs to later thermal events has also been found for Ru-Os-Ir alloys, laurite-erlichmanite and ruarsite-osarsite series PGM from ophiolite- and zoned-type massifs (Kostoyanov, 1998; Hattori and Cabri, 1992; Meibom et al., 2002; Malitch et al., 2003a; Pearson et al., 2007) and from Archaean paleoplacers of the Witwatersrand Basin, South Africa (Malitch and Merkle, 2004; Dale et al., 2010).

The highly restricted range of Os-isotope compositions found in both primary and secondary PGM assemblages at IPGE-rich localities in Shetland (Fig. 8, Table 5) and Nurali (Table 5) is at variance with the wider range of Os-isotope compositions recorded in ophiolitic primary PGM assemblages (i.e. containing Ru-Os-Ir alloys, laurite-erlichmanite and ruarsite-osarsite series PGM) from ophiolite-type complexes world-wide (e.g., Kostoyanov, 1998; Rudashevsky et al., 1999; Malitch et al., 2003a; Malitch, 2004; Ahmed et al., 2006; Shi et al., 2007; Nowell et al., 2008; Marchesi et al., 2011; González-Jiménez et al., 2012a, 2014; Badanina et al., 2014; Pašava et al., 2015 and references cited therein). The substantial Os isotope variability seen in the PGMs elsewhere was

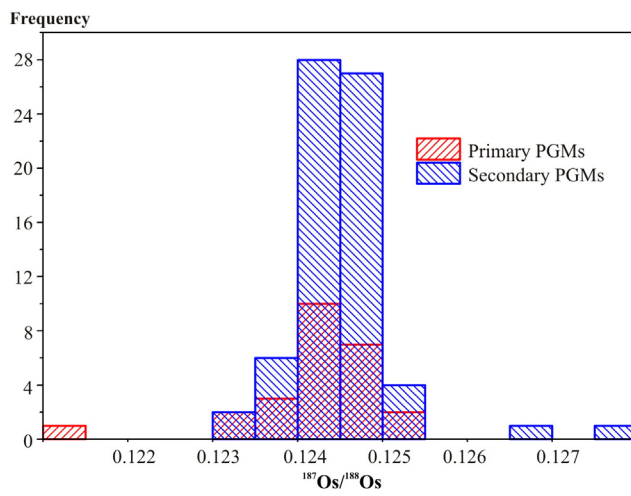


Fig. 8. Histogram of Os isotope compositions of primary and secondary PGMs from chromitite at Harold's Grave.

suggested as representing a long history of melting events of parent ultramafic source-rocks in the mantle (Malitch et al., 2003a; Malitch, 2004), supporting the conclusion that “the Os-isotope system of PGMs records multiple events during the chemical differentiation history of the mantle” (Carlson, 2002) controlled by deep geodynamic processes (Dobretsov and Kirdyashkin, 1998). Likewise, the Os-isotope data at Shetland and Nurali provide no further evidence of large-scale mantle heterogeneity in Os isotopes, as suggested previously (among others, Kostyanov, 1998; Malitch et al., 2003a; Pearson et al., 2007).

5.3. Os-isotope constraints on Re–Os models of the Earth's mantle and geodynamic implications

It has been shown (Luck and Allègre, 1991; Walker et al., 1996, 2002b; Tsuru et al., 2000) that Proterozoic and Phanerozoic ophiolites have broadly similar Os isotope signatures consistent with derivation from a chondritic mantle. Previous osmium isotope studies of the SOC were based solely on whole rock data (Walker et al., 2002b; O'Driscoll et al., 2012). Based on isotopic heterogeneity between chromitites and harzburgites O'Driscoll et al. (2012) argued that the former lithology might not be a suitable proxy for the average $^{187}\text{Os}/^{188}\text{Os}$ composition of the bulk convecting upper mantle. Since the geological history of the Shetland ophiolite is reasonably well-known (Spray, 1988; Flinn et al., 1991; Flinn, 2000, 2001, 2007; Flinn and Oglethorpe, 2005; Cutts et al., 2011, among others) the Os-isotope data can be used to constrain the long-term Re–Os evolution of the Earth's upper mantle. Different mantle evolution curves were defined as follows. The Carbonaceous Chondrite reservoir (CCR) curve assumes that the Earth's mantle has an Os isotopic composition and Re/Os similar to that of carbonaceous chondrites ($^{187}\text{Os}/^{188}\text{Os}_{\text{CC}} = 0.1262 \pm 0.0006$, $^{187}\text{Re}/^{188}\text{Os}_{\text{CC}} = 0.392 \pm 0.015$ (Walker et al., 2002a). The Enstatite Chondritic Reservoir (ECR) curve is calculated using a present-day $^{187}\text{Os}/^{188}\text{Os}$ value of 0.1281 ± 0.0004 and $^{187}\text{Re}/^{188}\text{Os} = 0.421 \pm 0.013$ as measured in enstatite chondrites (Walker et al., 2002a). The Primitive Upper Mantle (PUM) curve has a present day $^{187}\text{Os}/^{188}\text{Os} = 0.1296 \pm 0.0008$ and $^{187}\text{Re}/^{188}\text{Os} = 0.42$. These estimates were obtained through linear regression of suites of mantle-derived peridotite xenoliths and orogenic peridotites sampling mainly the Proterozoic to Phanerozoic subcontinental upper mantle (Meisel et al., 2001b). By comparing the Os-isotope composition of chromitite and distinct PGM assemblages and the independent chronological data available for the SOC we can distinguish between the various proposed mantle evolution curves (Fig. 9) following the approach of Shi et al. (2007). As is shown in Fig. 9 the CCR model yields an unrealistically young age (i.e. ca. 300 Ma), much younger than the emplacement age of the ophiolite. The PUM model would require melting (or depletion) at ca. 775 Ma, but that is older than the opening of Iapetus ocean system, so also seems unlikely. The ECR model would fit with melting at ca. 510–560 Ma, which is a reasonable match to the other available dating for the SOC, so seems most likely with the available data.

Using an ECR model we obtain Os-model ages ($T_{\text{MA}}^{\text{ECR}} - T_{\text{RD}}^{\text{ECR}}$) for PGM assemblages and chromitite within a range of ca. 508 and 580 Ma, respectively. These estimates would agree within the ECR model uncertainty (Fig. 9) with the plagiogranite zircon U-Pb ages (492 ± 3 Ma, Spray and Dunning, 1991) and the K-Ar ages of hornblende (465–479 Ma, Spray, 1988) determined in amphibolites found in Unst and Fetlar that are thought to be the remnants of dynamo-metamorphic sole from hot obduction (Williams and Smyth, 1973; Prichard, 1985), albeit one complicated by later tectonic and/or magmatic activity. Thus the unradiogenic $^{187}\text{Os}/^{188}\text{Os}$ isotope systematics of laurite-dominated assemblages in this study record melt depletion events that are slightly older than final crystallisation (i.e., of zircons from plagiogranites in late stage veins in the gabbro unit) and the subsequent ophiolite emplacement into crustal levels (i.e. metamorphic sole formation). Therefore, the ages implied by our modelling of these new Os isotope results are also consistent with a supra-subduction

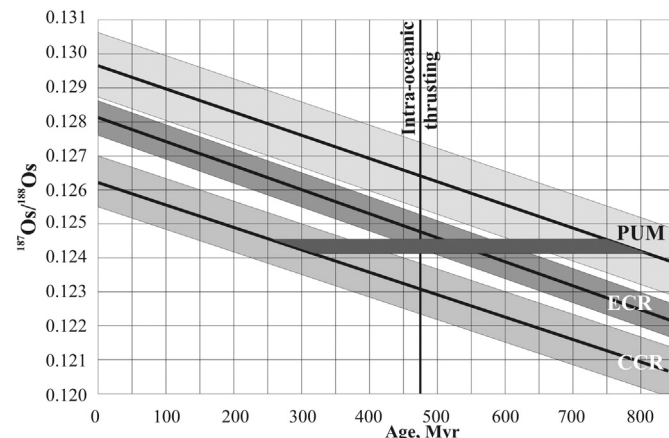


Fig. 9. Models for the Re–Os evolution of the convecting mantle (modified after Shi et al., 2007). Horizontal dark grey area corresponds to the osmium isotopic composition of PGM and chromitite from the Shetland massif.

zone origin of the SOC, which would be followed relatively rapidly by obduction.

6. Conclusions

1. Two distinct PGM assemblages (primary and secondary), each dominated by laurite and Os-rich alloy, have been observed at Harold's Grave in the Shetland Ophiolite Complex, below the transition zone harzburgite and petrological Moho. The primary PGM assemblage formed early (together with chromite), whereas the secondary PGM assemblage is likely to reflect alteration processes such as in-situ serpentinization, alteration during emplacement or regional greenschist metamorphism.
2. The osmium isotope results reveal broadly similar ‘unradiogenic’ $^{187}\text{Os}/^{188}\text{Os}$ values for both primary and secondary PGM assemblages which are similar to that of the chromitite host, supporting the conclusion that the ‘secondary’ PGMs preserved the subchondritic osmium isotope signature of the ‘primary’ PGMs. This implies that the whole-rock Os isotope budget is largely controlled by the laurite-dominant assemblages.
3. Os-isotope data for chromitite and the associated PGM assemblages support an ECR model for the convective upper mantle as defined by Walker et al. (2002b) and are consistent with origin of the complex as a Caledonian ophiolite formed in a supra-subduction zone shortly before obduction.
4. The results demonstrate that PGE-enriched ophiolite chromitites can still preserve primitive mantle Os isotope compositions, despite complex post-magmatic alteration histories.

Supplementary data to this article can be found online at <http://dx.doi.org/10.1016/j.oregeorev.2015.12.014>.

Conflict of interest

We do not have a conflict of interest for the manuscript “Closed-system behaviour of the Re–Os isotope system recorded in primary and secondary platinum-group mineral assemblages: evidence from a mantle chromitite at Harold's Grave (Shetland Ophiolite Complex, Scotland) by Inna Yu. Badanina, Kreshimir N. Malitch, Richard A. Lord, Elena A. Belousova and Thomas C. Meisel.”

Acknowledgements

This paper is a contribution to the grant #12-05-01166-a to I.Yu. Badanina funded by the Russian Foundation for Basic Research. The analytical data at CCFS/GEMOC were obtained using instrumentation

funded by ARC grant # FT110100685 to EAB. The chromitite sample used was originally collected by RAL as part of the Mining Industry Research Organisation research programme contract RC48. Prof. S.Y. O'Reilly, Prof. W.L. Griffin, Dr. J.M. González-Jiménez, Dr. N.J. Pearson, Dr. S.A. Junk, Dr. V.V. Knauf and Dr. H. Prichard are thanked for valuable discussions. This is contribution 679 from the ARC Centre of Excellence for Core to Crust Fluid Systems (<http://www.ccfs.mq.edu.au>) and 1042 in the GEMOC Key Centre (<http://www.gemoc.mq.edu.au>). The paper has benefitted from constructive comments of three anonymous reviewers. Careful editorial handling of Editor-in-chief Dr. Franco Pirajno is greatly appreciated.

References

- Ahmed, A.H., Hanghøj, K., Kelemen, P.B., Hart, S.R., Arai, S., 2006. Osmium isotope systematics of the Proterozoic and Phanerozoic ophiolitic chromitites: in-situ ion probe analysis of primary Os-rich PGM. *Earth Planet. Sci. Lett.* 245, 777–791.
- Akmaz, R.M., Uysal, I., Saka, S., 2014. Compositional variations of chromite and solid inclusions in ophiolitic chromitites from the southeastern Turkey: implications for chromite genesis. *Ore Geol. Rev.* 58, 208–224.
- Alard, O., Griffin, W.L., Pearson, N.J., Lorand, J.-P., O'Reilly, S.Y., 2002. New insights into the Re-Os systematics of sub-continenal lithospheric mantle from in situ analysis of sulphides. *Earth Planet. Sci. Lett.* 203, 651–663.
- Alard, O., Luguet, A., Pearson, N.J., Griffin, W.L., Lorand, J.-P., Gannoun, A., Burton, K.W., O'Reilly, S.Y., 2005. In situ os isotopes in abyssal peridotites bridge the isotopic gap between MORBs and their source mantle. *Nature* 436, 1005–1008.
- Andrews, D.R.A., Brenan, J.M., 2002. Phase-equilibrium constraints on the magmatic origin of laurite and Os-Ir alloy. *Can. Mineral.* 40, 1705–1716.
- Augé, T., 1985. Platinum-group-mineral inclusions in ophiolitic chromite from the Vourinos Complex, Greece. *Can. Mineral.* 23, 163–171.
- Augé, T., 1988. Platinum-group minerals in the Tiebaghi and Vourinos ophiolitic complexes: genetic implications. *Can. Mineral.* 26, 177–192.
- Augé, T., Johan, Z., 1988. Comparative study of chromite deposits from Troodos, Vourinos, North Oman and New Caledonia ophiolites. In: Boissonnas, J., Omenetto, P. (Eds.), *Mineral Deposits Within the European Community Special Publication of the Society for Geology Applied to Mineral Deposits*, Springer, Berlin, Heidelberg, pp. 267–288.
- Badanina, I.Y., Malitch, K.N., Lord, R.A., Meisel, T.C., 2013a. Origin of primary PGM assemblage in chromitite from a mantle tectonite at Harold's Grave (Shetland ophiolite complex, Scotland). *Mineral. Petrol.* 107, 963–970.
- Badanina, I.Y., Malitch, K.N., Murzin, V.V., Khiller, V.V., Glavatskikh, S.P., 2013b. Mineralogical and geochemical particularities of PGE mineralization of the Verkh-Neivinsk dunite-harzburgite massif (Middle Urals, Russia). *Proceedings of the Institute of Geology and Geochemistry UB RAS* 160, pp. 188–192 (in Russian).
- Badanina, I.Y., Malitch, K.N., Lord, R.A., Belousova, E.A., Griffin, W.L., Meisel, T.C., Murzin, V.V., Pearson, N.J., O'Reilly, S.Y., 2014. Mineral chemistry and isotopic composition of ophiolitic Os-rich alloys and Ru-Os sulfides: synthesis of new data. In: Anikina, E.V. et al. (Eds.), *12th International Platinum Symposium Abstracts*. Institute of Geology and Geochemistry UB RAS, Yekaterinburg, Russia, pp. 289–290.
- Barnes, S.J., Naldrett, A.J., Gorton, M.P., 1985. The origin of the fractionation of platinum-group elements in terrestrial magmas. *Chem. Geol.* 53, 303–323.
- Becker, H., Shirey, S.B., Carlson, R.W., 2001. Effects of melt percolation on the Re-Os systematics of peridotites from a Paleozoic convergent plate margin. *Earth Planet. Sci. Lett.* 188, 107–121.
- Brandon, A.D., Creaser, R.A., Shirey, S.B., Carlson, R.W., 1996. Osmium recycling in subduction zones. *Science* 272, 861–864.
- Brandon, A.D., Walker, R.J., Puchtel, I.S., 2006. Platinum-osmium isotope evolution of the Earth's mantle: constraints from chondrites and Os-rich alloys. *Geochim. Cosmochim. Acta* 70, 2093–2103.
- Brenan, J.M., Andrews, D., 2001. High-temperature stability of laurite and Ru-Os-Ir alloy and their role in PGE fractionation in mafic magmas. *Can. Mineral.* 39, 341–360.
- Brough, C.P., Prichard, H.M., Neary, C.R., Fisher, P.C., McDonald, I., 2015. Geochemical variations within podiform chromitite deposits in the Shetland ophiolite: implications for petrogenesis and PGE concentration. *Econ. Geol.* 110, 187–208.
- Burton, K.W., Schiano, P., Birck, J.-L., Allègre, C.J., 1999. Osmium isotope disequilibrium between mantle minerals in a spinel-lherzolite. *Earth Planet. Sci. Lett.* 172, 311–322.
- Burton, K.W., Gannoun, A., Birck, J.L., Allègre, C.J., Schiano, P., Clochiatti, R., Alard, O., 2002. The compatibility of rhenium and osmium in natural olivine and their behaviour during mantle melting and basalt genesis. *Earth Planet. Sci. Lett.* 198, 63–76.
- Carlson, R.W., 2002. Osmium remembers. *Science* 296, 475–477.
- Carlson, R.W., 2005. Application of the Pt-Re-Os isotopic systems to mantle geochemistry and geochronology. *Lithos* 82, 249–272.
- Corriveau, L., Laflamme, J.H.G., 1990. Minéralogie des éléments du groupe du platine dans les chromitites de l'ophiolite de Thetford Mines, Québec. *Can. Mineral.* 28, 579–595.
- Cutts, K.A., Hand, M., Kelsey, D.E., Strachan, R.A., 2011. P-T constraints and timing of Barrovian metamorphism in the Shetland Islands, Scottish Caledonides: implications for the structural setting of the Unst ophiolite. *J. Geol. Soc.* 168, 1265–1284.
- Dale, C.W., Pearson, D.G., Nowell, G.M., Parman, S.W., Oberthür, T., Malitch, K.N., 2010. Os isotopes in Witwatersrand platinum-group alloys: implications for ancient mantle melting events and the timing of gold formation. *Geochim. Cosmochim. Acta* 74 (12, Suppl. 1), A203.
- Derbyshire, E.J., O'Driscoll, B., Lenaz, D., Gertisser, R., Kronz, A., 2013. Compositionally heterogeneous podiform chromitite in the Shetland ophiolite complex (Scotland): implications for chromitite petrogenesis and late-stage alteration in the upper mantle portion of a supra-subduction zone ophiolite. *Lithos* 162–163, 279–300.
- Dick, H.J.B., Bullen, T., 1984. Chromian spinel as a petrogenetic indicator in abyssal and alpine-type peridotites and spatially associated lavas. *Contrib. Mineral. Petrol.* 86, 54–76.
- Dobretsov, N.L., Kirdyashkin, A.G., 1998. Deep-level geodynamics. *Swets and Zeitlinger, Rotterdam* (328 pp.).
- Flinn, D., 1985. The Caledonides of Shetland. In: Gee, D.G., Sturt, B.A. (Eds.), *The Caledonide Orogen - Scandinavia and related areas*. Wiley and Sons, pp. 1158–1171.
- Flinn, D., 1996. The Shetland ophiolite complex: field evidence for the intrusive emplacement of the 'cumulate' layers. *Scott. J. Geol.* 32, 151–158.
- Flinn, D., 2000. The architecture of the Shetland ophiolite complex. *Scott. J. Geol.* 36, 123–135.
- Flinn, D., 2001. The basic rocks of the Shetland ophiolite complex and their bearing on its genesis. *Scott. J. Geol.* 37, 79–96.
- Flinn, D., 2007. The Dalriadan rocks of Shetland and their implications for the plate tectonics of the northern Iapetus. *Scott. J. Geol.* 43, 125–142.
- Flinn, D., Oglesby, R.D., 2005. A history of the Shetland ophiolite complex. *Scott. J. Geol.* 41, 141–148.
- Flinn, D., Frank, P.L., Brook, M., Pringle, I.R., 1979. Basement-cover relations in Shetland. In: Harris, A., Holland, C.H., Leake, B.E. (Eds.), *The Caledonides of the British Isles Reviewed*. Geological Society, London, Spec. publ. 8, pp. 109–115.
- Flinn, D., Miller, J.A., Roddam, D., 1991. The age of the norwick hornblende schists of Unst and Fetlar and the obduction of the Shetland ophiolite. *Scott. J. Geol.* 27, 11–19.
- Garson, M.S., Plant, J., 1973. Alpine type ultramafic rocks and episodic mountain building in the Scottish Highlands. *Nat. Phys. Sci.* 242, 34–38.
- Garuti, G., Zaccarini, F., Moloshag, V., Alimon, V., 1999. Platinum-group minerals as indicators of sulfur fugacity in ophiolitic upper mantle: an example from chromitites of the Rai-Iz ultramafic complex, Polar Urals, Russia. *Can. Mineral.* 37, 1099–1115.
- González-Jiménez, J.M., Gervilla, F., Proenza, J.A., Augé, T., Kerestedjian, T., 2010. Distribution of platinum-group minerals in ophiolitic chromitites. *Trans. Inst. Min. Metall. Sect. B Appl. Earth Sci.* 118 (3–4), 101–110.
- González-Jiménez, J.M., Gervilla, F., Griffin, W.L., Proenza, J.A., Augé, T., O'Reilly, S.Y., Pearson, N.J., 2012a. Os-isotope variability within sulfides from podiform chromitites. *Chem. Geol.* 291, 224–235.
- González-Jiménez, J.M., Griffin, W.L., Gervilla, F., Kerestedjian, T.N., O'Reilly, S.Y., Proenza, J.A., Pearson, N.J., Sergeeva, I., 2012b. Metamorphism disturbs the Re-Os signatures of platinum-group minerals in ophiolitic chromitites. *Geology* 40, 659–662.
- González-Jiménez, J.M., Griffin, W.L., Gervilla, F., Proenza, J.A., O'Reilly, S.Y., Pearson, N.J., 2014. Chromitites in ophiolites: how, where, when, why? Part I. A review and new ideas on the origin and significance of platinum-group minerals. *Lithos* 189, 127–139.
- González-Jiménez, J.M., Locmelis, M., Belousova, E., Griffin, W., Gervilla, F., Kerestedjian, T.N., O'Reilly, S.Y., Pearson, N.J., Sergeeva, I., 2015. Genesis and tectonic implications of podiform chromitites in the metamorphosed ultramafic massif of Dobromiritsi (Bulgaria). *Gondwana Res.* 27, 555–574.
- Gunn, A.G., Leake, R.C., Styles, M.T., Bateson, J.H., 1985. Platinum-group element mineralisation in the Unst ophiolite, Shetland. *Mineral Reconnaissance Programme Report No. 73*. British Geological Survey, Keyworth UK, p. 116.
- Gunn, A.G., Styles, M.T., 2002. Platinum-group element occurrences in Britain: magmatic, hydrothermal and supergene. *Appl. Earth Sci. IMM Trans. Sect. B* 111, 2–14.
- Harris, D.C., Cabri, L.J., 1991. Nomenclature of platinum-group-element alloys: review and revision. *Can. Mineral.* 29, 231–237.
- Hart, S.R., Ravizza, G.E., 1996. Os partitioning between phases in lherzolite and basalt. In: Basu, A., Hart, S.R. (Eds.), *Earth Processes: Reading the Isotopic CodeGeophys. Monogr. Ser.* 95. AGU, Washington, USA, pp. 123–134.
- Hattori, K., Cabri, L.J., 1992. Origin of platinum-group mineral nuggets inferred from an osmium-isotope study. *Can. Mineral.* 30, 289–301.
- Hattori, K., Hart, S.R., 1991. Osmium-isotope ratios of platinum-group minerals associated with ultramafic intrusions: Os-isotopic evolution of the oceanic mantle. *Earth Planet. Sci. Lett.* 107, 499–514.
- Junk, S.A., 2001. Ancient artefacts and modern analytical techniques – usefulness of laser ablation ICP-MS demonstrated with ancient gold coins. *Nucl. Inst. Methods Phys. Res. B* 181, 723–727.
- Knauf, V.V., 1996. On the methodological background of mineralogical investigations. *Zap. Vser. Mineral. Obschch.* 125, 109–113 (in Russian).
- Kostyanov, A.I., 1998. Model Re-Os ages of platinum-group minerals. *Geol. Rudnykh Mestorozhdenii* 40, 545–550 (in Russian).
- Lago, B.L., Rabinowicz, M., Nicolas, A., 1982. Podiform chromite ore bodies: a genetic model. *J. Petrol.* 23, 103–125.
- Le Roux, V., Bodinier, J.-L., Alard, O., O'Reilly, S.Y., Griffin, W.L., 2009. Isotopic decoupling during porous melt flow: a case study in the Lherz peridotites. *Earth Planet. Sci. Lett.* 279, 76–85.
- Leblanc, M., 1991. Platinum-group elements and gold in ophiolitic complexes: distribution and fractionation from mantle to oceanic floor. In: Peters, T.J., Nicolas, A., Coleman, R.G. (Eds.), *Ophiolite Genesis and Evolution of the Oceanic Lithosphere*. Ministry of Petroleum and Minerals, Sultanate of Oman, pp. 231–260.
- Lorand, J.-P., Alard, O., 2001. Platinum-group element abundances in the upper mantle: new constraints from in situ and whole-rock analyses of Massif Central xenoliths (France). *Geochim. Cosmochim. Acta* 65, 2789–2806.
- Lord, R.A., 1991. Platinum-group element mineralisation in the Shetland ophiolite complex (Ph.D. thesis) Open University, Milton Keynes, U.K. (422 pp.).
- Lord, R.A., Prichard, H.M., 1997. Exploration and origin of stratigraphically controlled platinum-group element mineralization in crustal-sequence ultramafics, Shetland ophiolite complex. *Trans. Inst. Min. Metall. Sect. B Appl. Earth Sci.* 106, B179–B193.
- Lord, R.A., Prichard, H.M., Neary, C.R., 1994. Magmatic platinum-group element concentrations and hydrothermal upgrading in Shetland ophiolite complex. *Trans. Inst. Min. Metall. Sect. B* 103, 87–106.

- Luck, J.-M., Allègre, C.J., 1991. Osmium isotopes in ophiolites. *Earth Planet. Sci. Lett.* 107, 406–415.
- Luguet, A., Behrens, M., Pearson, D.G., Konig, S., Herwartz, D., 2015. Significance of the whole rock Re–Os ages in cryptically and modally metasomatised cratonic peridotites: constraints from HSE–Se–Te systematics. *Geochim. Cosmochim. Acta* 164, 441–463.
- Malitch, K.N., 2004. Osmium isotope constraints on contrasting sources and prolonged melting in the Proterozoic upper mantle: evidence from ophiolitic Ru–os sulfides and Ru–os–Ir alloys. *Chem. Geol.* 208, 157–173.
- Malitch, K.N., Merkle, R.K.W., 2004. Ru–Os–Ir–Pt and Pt–Fe alloys from the Evander Goldfield (Witwatersrand Basin, South Africa): detrital origin inferred from compositional and osmium isotope data. *Can. Mineral.* 42, 631–650.
- Malitch, K.N., Melcher, F., Mühlhans, H., 2001. Palladium and gold mineralization in podiform chromitite at Kraubath, Austria. *Mineral. Petrol.* 73, 247–277.
- Malitch, K.N., Augé, T., Badanina, I.Y., Goncharov, M.M., Junk, S.A., Pernicka, E., 2002. Osmium nuggets from Au–PGE placers of the Maimecha–Kotui Province, Russia: a multidisciplinary study. *Mineral. Petrol.* 76, 121–148.
- Malitch, K.N., Junk, S.A., Thalhammer, O.A.R., Melcher, F., Knauf, V.V., Pernicka, E., Stumpf, E.F., 2003a. Laurite and ruarsite from podiform chromitites at Kraubath and Hochgrussen, Austria: new insights from osmium isotopes. *Can. Mineral.* 41, 331–352.
- Malitch, K.N., Thalhammer, O.A.R., Knauf, V.V., Melcher, F., 2003b. Diversity of platinum-group mineral assemblages in banded and podiform chromitite from the Kraubath ultramafic massif, Austria: evidence for an ophiolitic transition zone? *Mineral. Deposita* 38, 282–297.
- Malitch, K.N., Anikina, E.V., Badanina, I.Y., Belousova, E.A., Griffin, W.L., Khiller, V.V., Pearson, N.J., Pushkarev, E.V., O'Reilly, S.Y., 2014. Closed-system behaviour of the Re–Os isotope system in primary and secondary PGM assemblages: evidence from the Nurali ultramafic complex (Southern Urals, Russia). In: Anikina, E.V., et al. (Eds.), 12th International Platinum Symposium Abstracts. Institute of Geology and Geochemistry UB RAS, Yekaterinburg, Russia, pp. 299–300.
- Malitch, K.N., Anikina, E.V., Badanina, I.Y., Belousova, E.A., Pushkarev, E.V., Khiller, V.V., 2016. Composition and osmium isotope systematics of primary and secondary platinum-group mineral assemblages from Mg-bearing chromitite of the Nurali Iherzolite massif (Russia). *Geol. Ore Deposits* 58 (1) (in press).
- Marchesi, C., González-Jiménez, J.M., Gervilla, F., Griffin, W.L., O'Reilly, S.Y., Proenza, J.A., Pearson, N.J., 2011. In situ Re–Os isotopic analysis of platinum-group minerals from the Mayarí–Cristal ophiolitic massif (Mayarí–Baracoa Ophiolitic Belt, eastern Cuba): implications for the origin of Os-isotope heterogeneities in podiform chromitites. *Contrib. Mineral. Petrol.* 161, 977–990.
- Martin, C.E., Papanaftassiou, D.A., Wasserburg, G.J., Peach, C.L., 1993. Os isotopic composition of sulfide globules from MORB. *EOS Trans. Am. Geophys. Union* 74, 121.
- McDonough, W.F., Sun, S.S., 1995. The composition of the Earth. *Chem. Geol.* 120, 223–253.
- Meibom, A., Sleep, N.H., Chamberlain, C.P., Coleman, R.G., Frei, R., Hren, M.T., Wooden, J.L., 2002. Re–Os isotopic evidence for long-lived heterogeneity and equilibration processes in the Earth's upper mantle. *Nature* 419, 705–708.
- Meisel, T., Moser, J., Fellner, N., Wegscheider, W., Schoenberg, R., 2001a. Simplified method for the determination of Ru, Pd, Re, Os, Ir and Pt in chromitites and other geological materials by isotope dilution ICPMS and acid digestion. *Analyst* 126, 322–328.
- Meisel, T., Walker, R.J., Irving, A.J., Lorand, J.-P., 2001b. Osmium isotopic composition of mantle xenoliths: a global perspective. *Geochim. Cosmochim. Acta* 65, 1311–1323.
- Meisel, T., Fellner, N., Moser, J., 2003. A simple procedure for the determination of platinum-group elements and rhenium (Ru, Pd, Re, Os, Ir and Pt) using ID-ICP-MS with an inexpensive on-line–matrix separation in geological and environmental materials. *J. Anal. At. Spectrom.* 18, 720–726.
- Melcher, F., 2000. Chromite and platinum-group elements as indicators of mantle petrogenesis. (Unpubl. Habil. thesis) Mining University Leoben (202 pp.).
- Melcher, F., Grun, W., Simon, G., Thalhammer, T.V., Stumpf, E.F., 1997. Petrogenesis of the ophiolitic giant chromite deposits of Kempirsai, Kazakhstan: a study of solid and fluid inclusions in chromite. *J. Petrol.* 38, 1419–1458.
- Nakagawa, M., Franco, H.A., 1997. Placer Os–Ir–Ru alloys and sulfides: indicators of sulfur fugacity in an ophiolite. *Can. Mineral.* 35, 1441–1452.
- Nowell, G.M., Pearson, D.G., Parman, S.W., Luguet, A., Hanski, E., 2008. Precise and accurate $^{186}\text{Os}/^{188}\text{Os}$ and $^{187}\text{Os}/^{188}\text{Os}$ measurements by multi-collector plasma ionisation mass spectrometry, part II: laser ablation and its application to single-grain Pt–Os and Re–Os geochronology. *Chem. Geol.* 248, 394–426.
- O'Driscoll, B., James, M.D., Day, J.M.D., Walker, R.J., Daly, J.S., McDonough, W.F., Piccoli, P.M., 2012. Chemical heterogeneity in the upper mantle recorded by peridotites and chromitites from the Shetland ophiolite complex, Scotland. *Earth Planet. Sci. Lett.* 333–334, 226–237.
- O'Reilly, S.Y., Griffin, W.L., 2012. Mantle metasomatism. In: Harlov, D.E., Austrheim, H. (Eds.), Metasomatism and the Chemical Transformation of Rock: Lecture Notes in Earth System Sciences. Springer-Verlag, Berlin, pp. 467–528.
- Paliulionyte, V., Meisel, T., Ramminger, P., Kettisch, P., 2006. High pressure asher digestion and an isotope dilution-ICP-MS method for the determination of platinum-group element concentrations in chromitite reference materials CHR-Bkg, GAN Pt-1 and HHH. *Geostand. Geoanal. Res.* 30, 87–96.
- Pašava, J., Malec, J., Griffin, W.L., González-Jiménez, J.M., 2015. Re–Os isotopic constraints on the source of platinum-group minerals (PGMs) from the vestřev pyrope-rich garnet placer deposit, Bohemian Massif. *Ore Geol. Rev.* 68, 117–126.
- Pearson, N.J., Alard, O., Griffin, W.L., Jackson, S.E., O'Reilly, S.Y., 2002. In situ measurement of Re–Os isotopes in mantle sulfides by laser ablation multicollector-inductively coupled plasma mass spectrometry: analytical methods and preliminary results. *Geochim. Cosmochim. Acta* 66, 1037–1050.
- Pearson, D.G., Parman, S.W., Nowell, G.M., 2007. A link between large mantle melting events and continent growth seen in osmium isotopes. *Nature* 449, 202–205.
- Prichard, H.M., 1985. The Shetland Ophiolite. In: Gee, D.G., Sturt, B.A. (Eds.), The Caledonide Orogen: Scandinavia and Related Areas 2. Wiley and Sons. Ltd., pp. 1173–1184.
- Prichard, H.M., Lord, R.A., 1988. The Shetland ophiolite: evidence for a supra-subduction zone origin and implications for platinum-group element mineralization. In: Boissonnas, J., Omenetto, P. (Eds.), Mineral Deposits within the European Community Special Publication No. 6 of the Society for Geology Applied to Mineral Deposits. Springer-Verlag, Berlin, pp. 289–302.
- Prichard, H.M., Lord, R.A., 1993. An overview of the PGE concentrations in the Shetland ophiolite complex. In: Prichard, H.M., Alabaster, T., Harris, N.B.W., Neary, C.R. (Eds.), Magmatic Processes and Plate Tectonics. Special Publication of the Geological Society of London 76, pp. 273–294.
- Prichard, H.M., Tarkian, M., 1988. Platinum and palladium minerals from two PGE-localities in the Shetland ophiolite complex. *Can. Mineral.* 26, 979–990.
- Prichard, H.M., Neary, C.R., Potts, P.J., 1986. Platinum-group minerals in the Shetland ophiolite. In: Gallagher, M.J., Ixer, R.A., Neary, C.R., Prichard, H.M. (Eds.), Metallogeny of Basic and Ultrabasic Rocks. Inst. Mining Metall., London, pp. 395–414.
- Prichard, H.M., Ixer, R.A., Lord, R.A., Maynard, J., Williams, N., 1994. Assemblages of platinum-group minerals and sulfides in silicate lithologies and chromite-rich rocks within the Shetland ophiolite. *Can. Mineral.* 32, 271–294.
- Prichard, H.M., Lord, R.A., Neary, C.R., 1996. A model to explain the occurrence of platinum- and palladium-rich ophiolite complexes. *J. Geol. Soc.* 153, 323–328.
- Prichard, H.M., Neary, C.R., Fisher, P.C., O'Hara, M.J., 2008. PGE-rich podiform chromitites in the Al'Ay ophiolite complex, Saudi Arabia: an example of critical mantle melting to extract and concentrate PGE. *Econ. Geol.* 103, 1507–1529.
- Reisberg, L., Lorand, J.-P., Bedini, R.M., 2004. Reliability of Os model ages in pervasively metasomatized continental mantle lithosphere: a case study of Sidamo spinel peridotite xenoliths (East African Rift, Ethiopia). *Chem. Geol.* 208, 119–140.
- Rosman, K.J.R., Taylor, P.D.P., 1998. Isotopic compositions of the elements 1997. Pure Appl. Chem. 70, 217–235.
- Rudashevsky, N.S., Kostyanov, A.I., Rudashevsky, V.N., 1999. Mineralogical and isotope evidences of origin of the Alpine-type massifs (the Ust'-Bel'sky massif, Koryak Highland, as an example). *Zap. Vser. Mineral. Obshch.* 128, 11–28 (in Russian).
- Rudashevsky, N.S., Garuti, G., Andersen, J.C.Ø., Kretser, Y.L., Rudashevsky, V.N., Zaccarini, F., 2002. Separation of accessory minerals from rocks and ores by hydroseparation (HS) technology: method and application to CHR-2 chromitite, Niquelandia, Brazil. *Transactions, Institution of Mining and Metallurgy, Proceedings Australasian Institute of Mining Metallurgy (Sect. B: Applied earth science)* 111, pp. B87–B94.
- Rudnick, R.L., Walker, R.J., 2009. Interpreting ages from Re–Os isotopes in peridotites. *Lithos* 112, 1083–1095.
- Sambridge, M., Lambert, D.D., 1997. Propagating errors in decay equations: examples from the Re–Os isotopic system. *Geochim. Cosmochim. Acta* 61, 3019–3024.
- Shi, R., Alard, O., Zhi, X., O'Reilly, S.Y., Pearson, N.J., Griffin, W.L., Zhang, M., Chen, X., 2007. Multiple events in the Neo-Tethyan oceanic upper mantle: evidence from Ru–Os–Ir alloys in the Luobusa and Dongqiao ophiolitic podiform chromitites, Tibet. *Earth Planet. Sci. Lett.* 261, 33–48.
- Shirey, S.B., Walker, R.J., 1998. The Re–Os isotope system in cosmochemistry and high-temperature geochemistry. *Annu. Rev. Earth Planet. Sci.* 26, 423–500.
- Smoliar, M.I., Walker, R.J., Morgan, J.W., 1996. Re–Os ages of group IIA, IIIA, IVA, and IVB meteorites. *Science* 271, 1099–1102.
- Spray, J.G., 1988. Thrust related metamorphism beneath the Shetland islands ocean fragment, north-east Scotland. *Can. J. Earth Sci.* 25, 1770–1776.
- Spray, J.G., Dunning, G.R., 1991. A U/Pb age for the Shetland islands oceanic fragment, Scottish Caledonides: evidence from anatectic plagiogranites in 'layer 3' shear zones. *Geol. Mag.* 128, 667–671.
- Standish, J.J., Hart, S.R., Blusztajn, J., Dick, H.J.B., Lee, K.L., 2001. Abyssal peridotite osmium isotopic compositions from Cr-spinel. *Geochim. Geophys. Geosyst.* 3 (1), 2002. <http://dx.doi.org/10.1029/2001GC000161>.
- Tarkian, M., Prichard, H., 1987. Irarsite–hollyingworthite solid solution series and other associated Os-, Ir- and Rh-bearing PGM's from the Shetland ophiolite complex. *Mineral. Deposita* 22, 178–184.
- Tessalina, S.G., Bourdon, B., Gannoun, A., Campas, F., Birck, J.-L., Allegre, C.J., 2007. Complex proterozoic to paleozoic history of the upper mantle recorded in the Urals Iherzolite massifs by Re–Os and Sm–Nd systematics. *Chem. Geol.* 240, 61–84.
- Torres-Ruiz, J., Garuti, G., Gazzotti, M., Gervilla, F., Fenoli Hach-Ali, P., 1996. Platinum-group minerals in chromitites from the Ojen Iherzolite massif (Serranía de Ronda, Betic Cordillera, Southern Spain). *Mineral. Petrol.* 56, 25–50.
- Tsuru, A., Walker, R.J., Kontinen, A., Peltonen, P., Hanski, E., 2000. Re–Os isotopic systematics of the 1.95 Ga Jormua ophiolite complex, northeastern Finland. *Chem. Geol.* 164, 123–141.
- Walker, R.J., Hanski, E., Vuollo, J., Liipo, J., 1996. The Os isotopic composition of Proterozoic upper mantle: evidence from the Outokumpu ophiolite, Finland. *Earth Planet. Sci. Lett.* 141, 161–173.
- Walker, R.J., Horan, M.F., Morgan, J.W., Becker, H., Grossman, J.N., Rubin, A.E., 2002a. Comparative $^{187}\text{Re}–^{187}\text{Os}$ systematics of chondrites: implications regarding early solar system processes. *Geochim. Cosmochim. Acta* 66, 4187–4201.
- Walker, R.J., Prichard, H.M., Ishiwatari, A., Pimentel, M., 2002b. The osmium isotopic composition of convecting upper mantle deduced from ophiolite chromites. *Geochim. Cosmochim. Acta* 66, 329–345.
- Williams, H., Smyth, W.R., 1973. Metamorphic aureoles beneath ophiolite suites and Alpine peridotites: tectonic implications with west Newfoundland examples. *Am. J. Sci.* 273, 594–621.